Electronic Supplementary Material (ESI) for Nanoscale Horizons.

Supporting Information for

“Selective visible-light driven highly efficient photocatalytic reduction of CO_2 to C_2H_5OH by two-dimensional Cu_2S monolayers”

Shiyan Wang, Xiaowan Bai, Qiang Li, Yixin Ouyang, Li Shi and Jinlan Wang*

School of Physics, Southeast University, Nanjing 211189, China.

*E-mail: jlwang@seu.edu.cn

Computational details

The binding energy, $E_b(CO)$ and $E_b(CHO)$, is defined as

$$E_b(CO) = E(CO^*) - E^* - E[CO_{(g)}]$$

$$E_b(CHO) = E(CHO^*) - E^* - E[CO_{(g)})] - \frac{1}{2}E[H_{2(g)}]$$

where E^*, $E[_{(g)}]$ and $E(^*)$ represent the total energies of the clean slab, the isolated adsorbed molecule and the slab after adsorption, respectively.

The Gibbs free energy change (ΔG) of each elementary reaction was calculated as

$$\Delta G = \Delta E + \Delta E_{ZPE} - T\Delta S + \Delta G_{pH} + \Delta G_U + \int C_P dT$$

where ΔE is the total energy difference directly obtained from DFT calculations, ΔE_{ZPE} is the change in zero-point energies, T is the temperature, ΔS is the entropy change and C_P is the heat capacity. $\Delta G_U = -neU$, where n is the number of ($H^+ + e^-$) pairs transferred in CO_2RR and U is the electrode potential versus the reversible hydrogen electrode (RHE). ΔG_{pH} is the correction of the H^+ free energy by the concentration, $\Delta G_{pH} = k_BT \times \ln 10 \times pH$, where k_B is the Boltzmann constant, and the value of pH was set to be zero for acidic condition. Zero-point energies and entropies of the CO_2RR intermediates were computed from the vibrational frequencies.

The limiting potential U_L was obtained from the maximum free energy change (ΔG_{max}) of the whole reaction process by using the relation $U_L = -\Delta G_{max}/e$.

The energy barrier of $E_{barrier}$ was calculated according to the following formula

$$E_{barrier} = E_{TS} - E_{IS}$$

where E_{TS} and E_{IS} are energies of the transition state and initial state, respectively.

The optical absorption coefficient $\alpha(\omega)$ was calculated from the following relation:

$$\alpha(\omega) = \sqrt{2}\frac{\omega}{c}\left[\sqrt{\varepsilon_1^2(\omega) + \varepsilon_2^2(\omega)} - \varepsilon_1(\omega)\right]^{1/2}$$

where $\varepsilon_1(\omega)$ and $\varepsilon_2(\omega)$ are the real part and imaginary part of dielectric function, respectively. The imaginary part of dielectric function is selected as the optical absorption.

The conduction band minimum (CBM) and valence band maximum (VBM) edge positions of Cu_2S catalysts with respect to NHE were calculated by using the following equations:

$$E_{CBM} = - \Phi + 0.5E_g$$

$$E_{VBM} = - \Phi - 0.5E_g$$

$$E'_{CBM/VBM} = - E_{CBM/VBM} - 4.45$$

where Φ is the work function, E_g is the band gap, $E'_{CBM/VBM}$ represent energy levels relative to NHE.

Zero-point energy (ZPE) and entropy corrections (TS)

The entropies of the gaseous molecules were taken from the NIST Chemistry WebBook and the zero-point energy (ZPE) was calculated according to:

$$E_{ZPE} = \sum_{i=1}^{3N} \frac{hv_i}{2}$$

The entropy change for adsorbed intermediates was calculated within the harmonic approximation:

$$\Delta S_{ads}(0 \rightarrow T, P^0) = S_{vib} = \sum_{i=1}^{3N} \left[\frac{N_A hv_i}{T(e^{hv_i/K_BT} - 1)} - R\ln\left(1 - e^{-hv_i/K_BT}\right) \right]$$

Where ν_i is DFT-calculated normal-mode frequency for species of *3N* degree of freedom (*N*=number of atoms) adsorbed on Cu_2S monolayers, N_A is the Avogadro's constant (6.022 × 10^{23} mol^{-1}), *h* is the Planck's constant (6.626 × 10^{-34}J s), and k_B is the Boltzmann constant (1.38 × 10^{-23} JK^{-1}), *R* is the ideal gas constant (8.314 J K^{-1} mol^{-1}), and *T* is the system temperature, and *T*=298K in this work. The energy corrections of gas-phase species, including zero point energies and entropies, are listed below:

Table S1. Free energy corrections for gas-phase species.

Molecule	ZPE (eV)	TΔS (eV)
CO_2	0.31	0.66
CO	0.13	0.61
H_2	0.28	0.40
H_2O	0.57	0.67
C_2H_4	1.36	0.71
C_2H_5OH	2.11	0.83

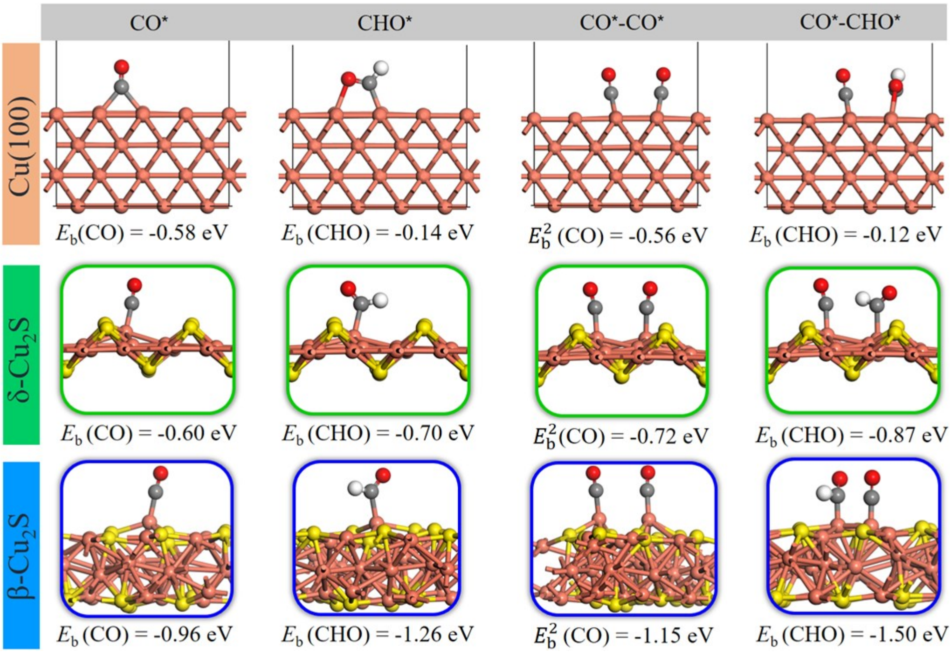

Figure S1. Optimized geometries of CO* and CHO* adsorbed on Cu(100), δ-Cu_2S and β-Cu_2S. Binding energies of CHO* and CO* also shown in the Figure. $E_b^2(CO)$ represent the binding energy of the second carbon monoxide.

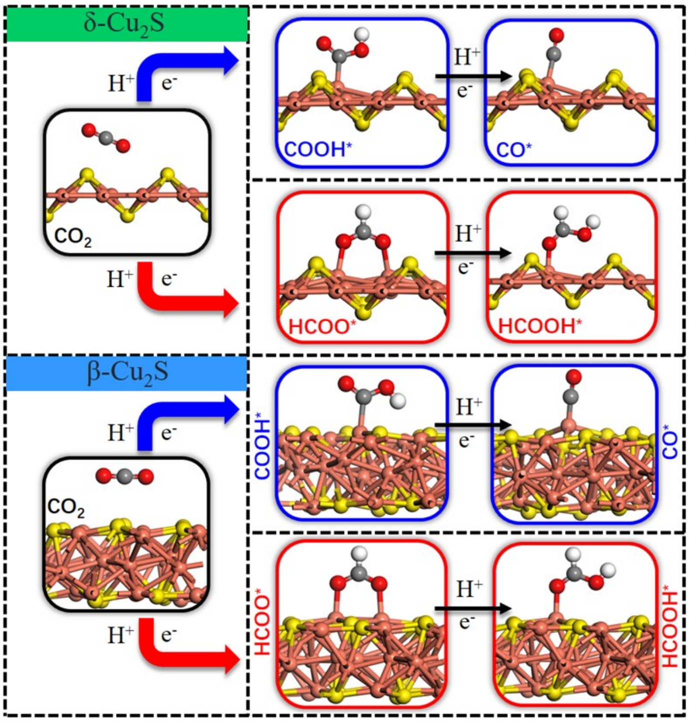

Figure S2. Optimized geometric of various intermediates along the most favorable two paths: Ⅰ) CO_2→COOH*→CO*; Ⅱ) CO_2→HCOO*→HCOOH* in the CO_2RR proceeded on δ-Cu_2S and β-Cu_2S when two proton/electron pairs ($H^+ + e^-$) are transferred.

Table S2. The free energy of CO_2 hydrogenation to CO* and HCOOH* on δ-Cu_2S and β-Cu_2S.

	CO_2	$COOH^*/HCOO^*$	$CO^*+H_2O/HCOOH^*$
δ-Cu_2S	0.00	0.21/−0.56	−0.86/−0.10
β-Cu_2S	0.00	0.08/−0.44	−0.71/−0.01

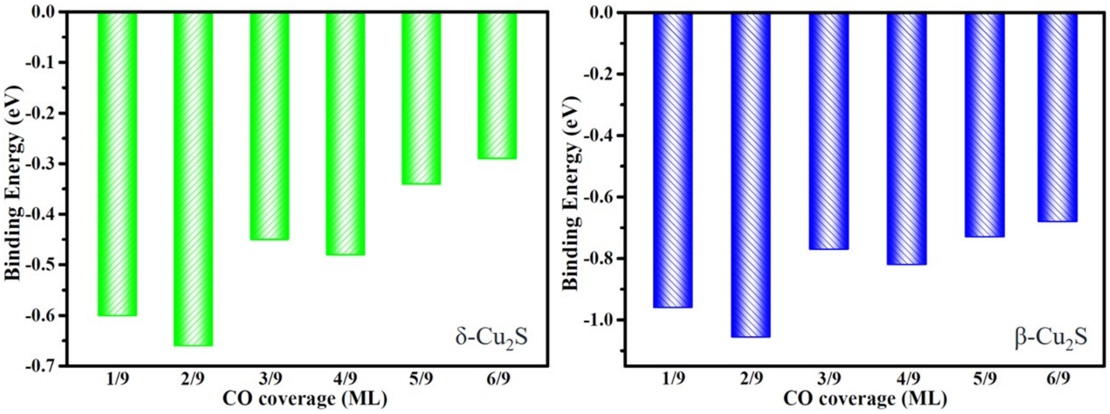

Figure S3. The relation between the CO coverage and the binding energies for δ-Cu_2S and β-Cu_2S.

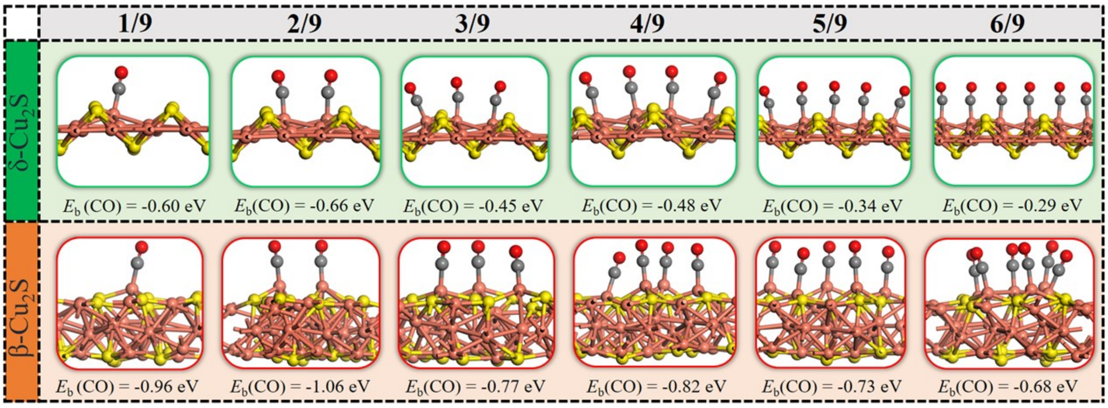

Figure S4. Detailed adsorption configurations and binding energies of CO molecule for different surface coverage.

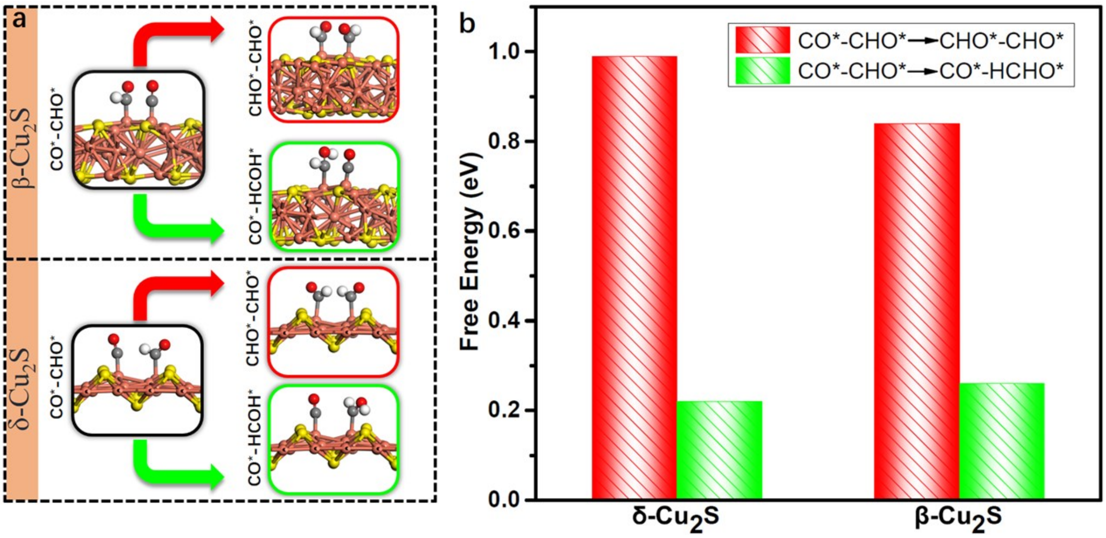

Figure S5. (a) Optimized geometric of various intermediates along the most favorable two paths: Ⅰ) CO*-CHO*→CHO*-CHO*; Ⅱ) CO*-CHO*→CO*-HCOH*. **(b)** Free energy of the hydrogenation of CO*-CHO* into CHO*-CHO* and CO*-HCOH* on δ-Cu$_2$S and β-Cu$_2$S.

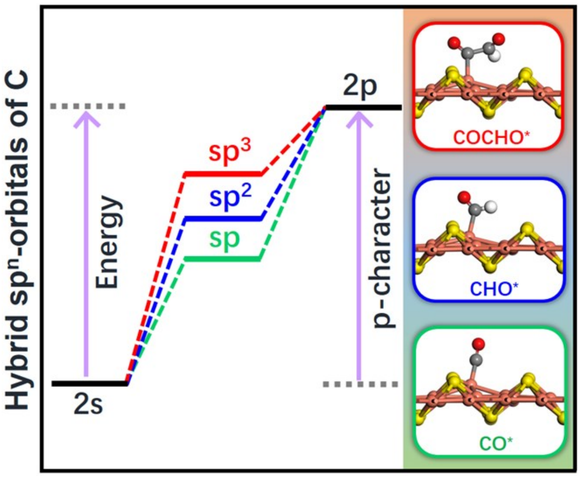

Figure S6. Schematic molecular orbital energy diagram for sp^n (n = 1, 2 and 3) hybridization of C atom in CO*, CHO* and COCHO* species.

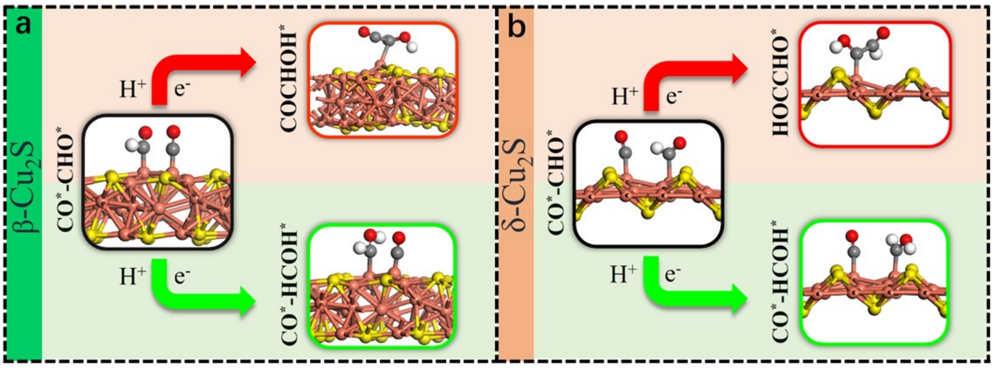

Figure S7. Optimized geometric of the intermediates along C$_1$ path: CO*-CHO*→CHO*-HCOH*; C$_2$ path: CO*-CHO*→COCHOH*/HOCCHO* on **(a)** β-Cu$_2$S and **(b)** δ-Cu$_2$S.

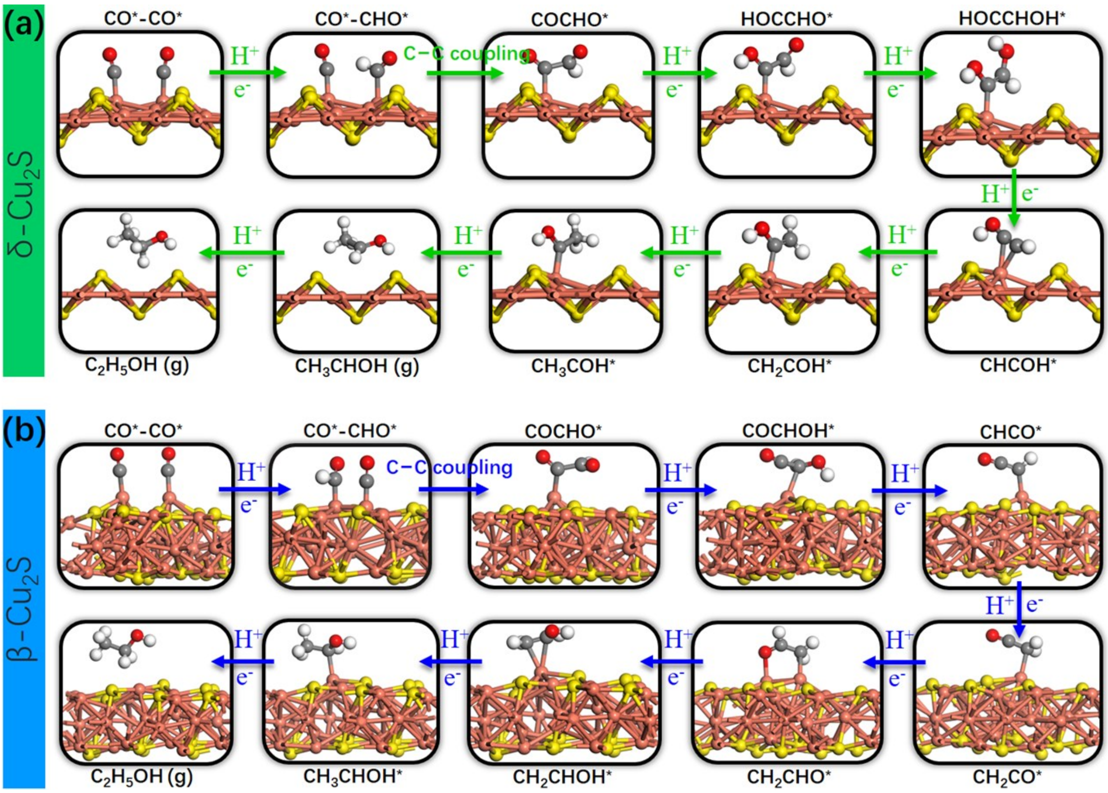

Figure S8. Optimized geometric of various intermediates of CO*-CO*, CO*-CHO*, COCHO*, HOCCHO*, HOCCHO*, CHCOH*, CH_2COH*, CH_3CHO*, CH_3CHOH and C_2H_5OH on the **(a)** δ-Cu_2S surface; and CO*-CO*, CO*-CHO*, COCHO*, COCHOH*, CHCO*, CH_2CO*, CH_2CHO*, CH_2CHOH*, CH_3CHOH and C_2H_5OH on the **(b)** β-Cu_2S surface along the reaction path of CO_2RR proceeded.

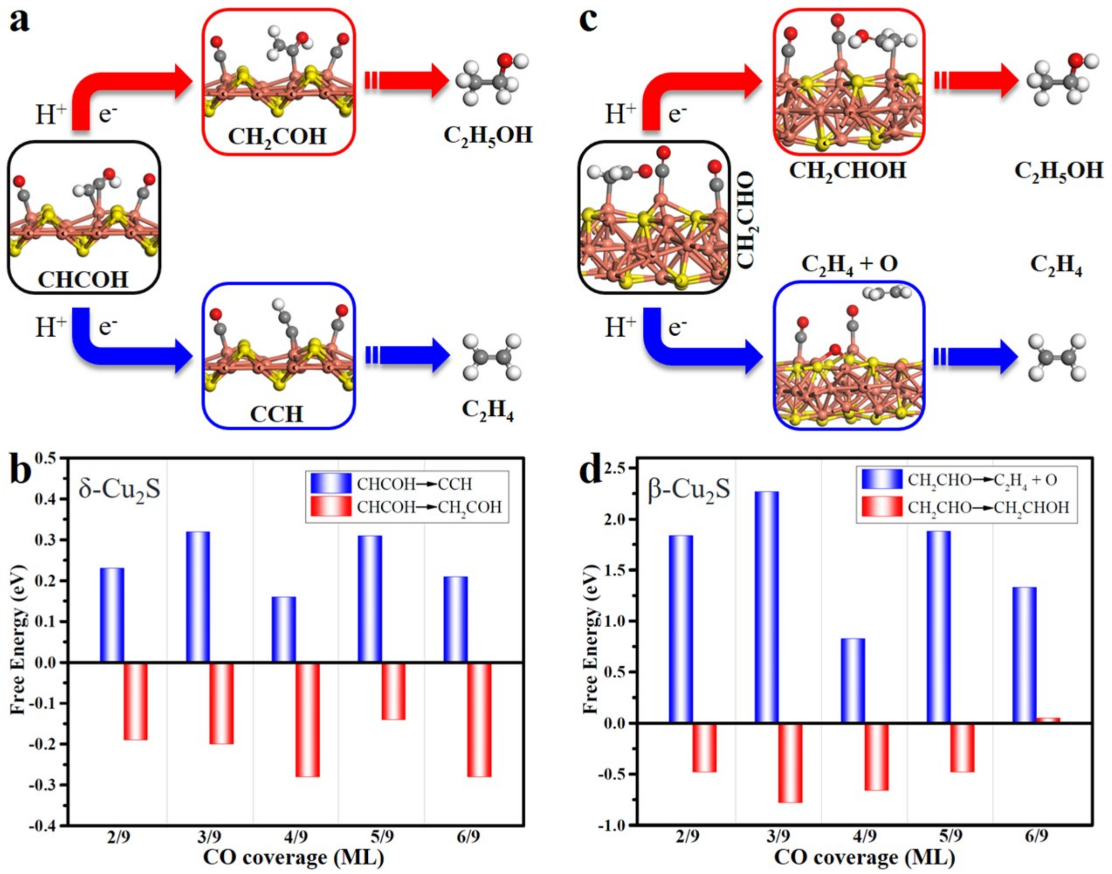

Figure S9. Key reaction pathways for **(a)** $CHCOH^* \rightarrow CH_2COH^*$ (ethanol path) or $CHCOH^* \rightarrow CCH^*$ (ethylene path) on δ-Cu_2S surface; **(c)** $CH_2CHO^* \rightarrow CH_2CHOH^*$ (ethanol path) or $CH_2CHO^* \rightarrow C_2H_4$ (ethylene path) on β-Cu_2S surface. Reaction free energies of **(b)** $CHCOH^* \rightarrow CH_2COH^*$ or $CHCOH^* \rightarrow CCH^*$ on δ-Cu_2S surface; and **(d)** $CH_2CHO^* \rightarrow CH_2CHOH^*$ or $CH_2CHO^* \rightarrow C_2H_4$ on β-Cu_2S surface under different CO* coverages ranging from 2/9 to 6/9 monolayer (ML).

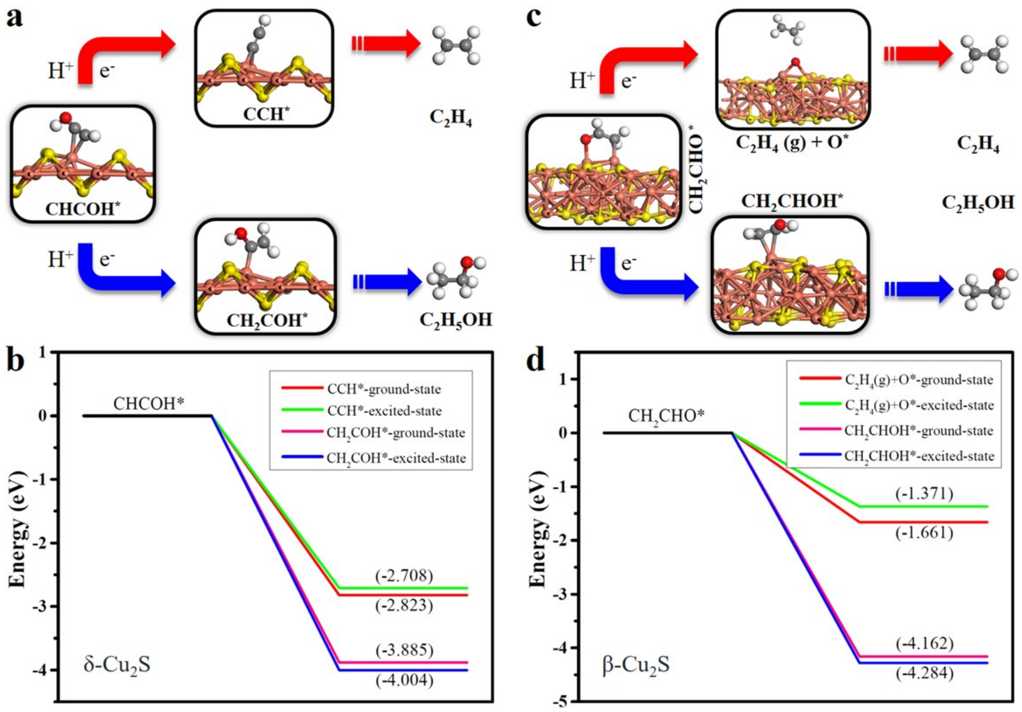

Figure S10. Key reaction pathways for **(a)** CHCOH*→CH_2COH* (ethanol path) or CHCOH*→ CCH* (ethylene path) on δ-Cu_2S surface, **(c)** CH_2CHO*→CH_2CHOH* (ethanol path) or CH_2CHO* →C_2H_4 (ethylene path) on β-Cu_2S surface. Energy profiles for **(b)** CHCOH*→CCH* or CHCOH* →CH_2COH* on δ-Cu_2S surface, and **(d)** CH_2CHO*→C_2H_4 or CH_2CHO*→CH_2CHOH* on β-Cu_2S surface under the electro-driven (ground-state) and photo-driven (excited-state).

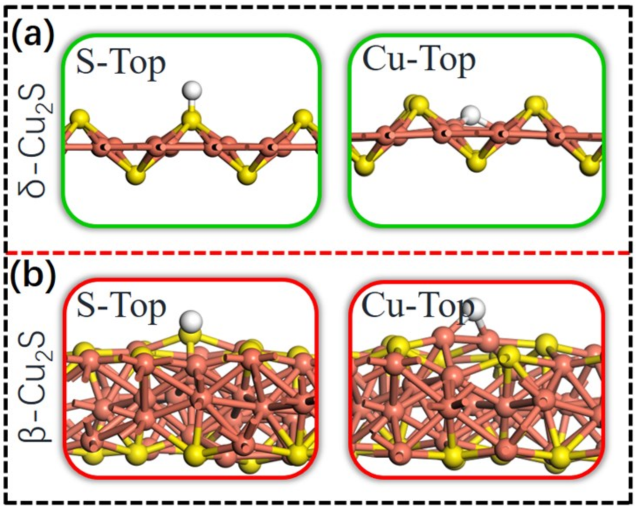

Figure S11. Optimized geometries of H* adsorbed on **(a)** δ-Cu_2S and **(b)** β-Cu_2S.

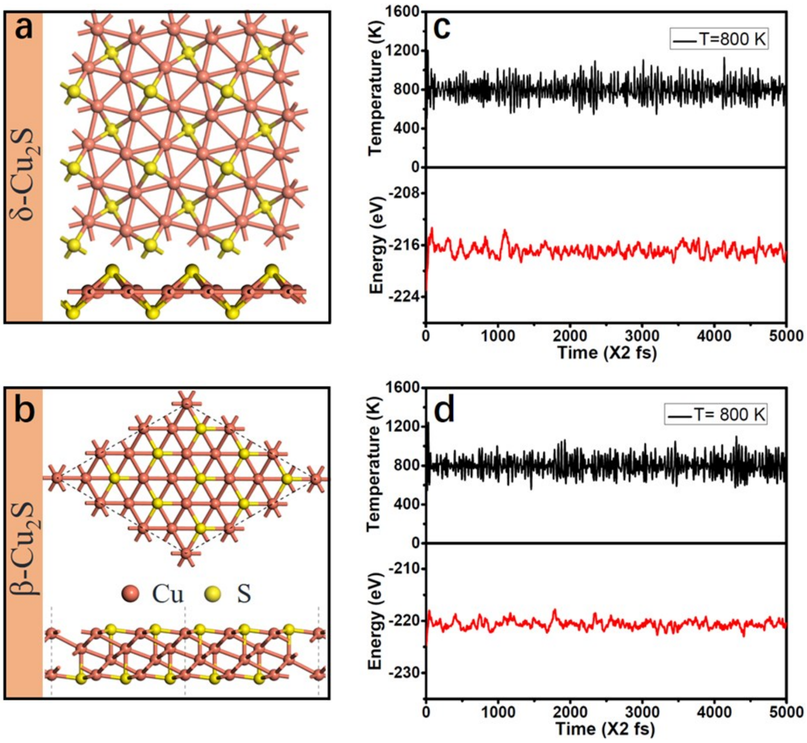

Figure S12. Top and side views of atomic configurations of **(a)** δ-Cu_2S and **(b)** β-Cu_2S in a 3 × 3 supercell. Color scheme: pink and yellow spheres represent Cu and S atoms, respectively. Variations of temperature and energy fluctuations versus AIMD simulation time progress for **(c)** δ-Cu_2S and **(d)** β-Cu_2S. The simulation lasting for 10 ps with a time step of 2 fs at $T = 800$ K.

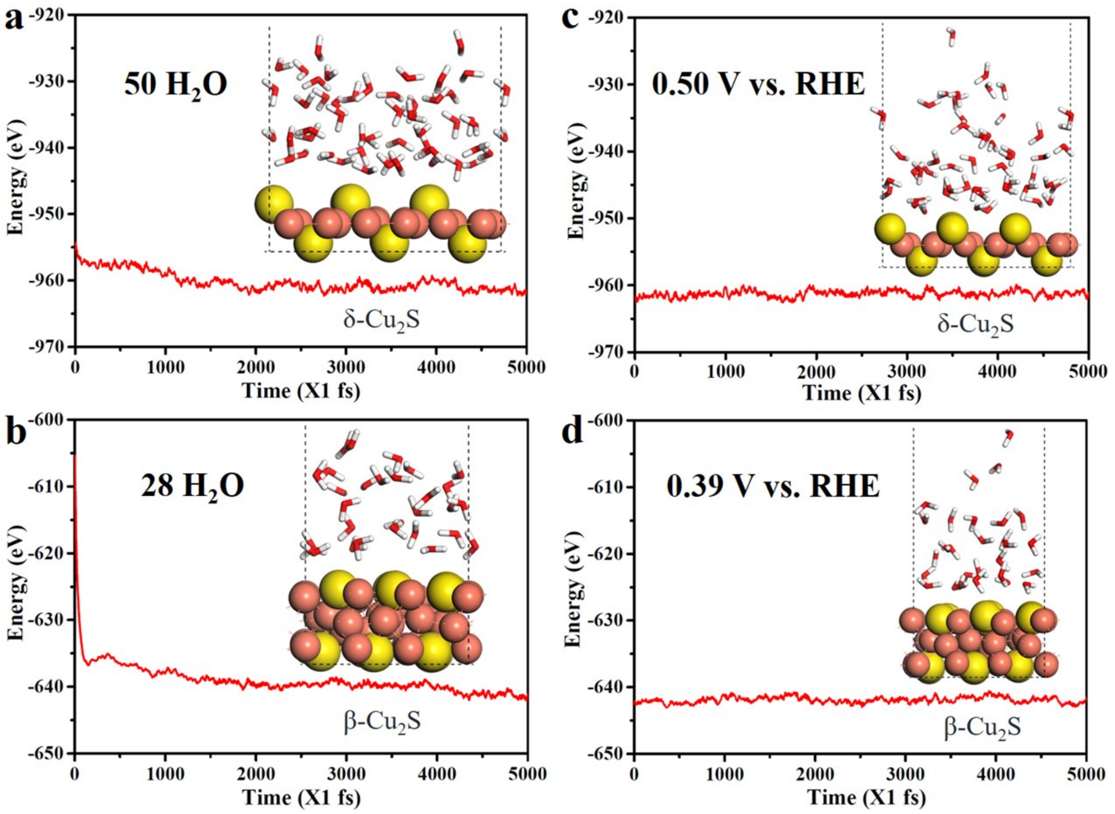

Figure S13. Energy fluctuations versus AIMD simulation time progress under the existence of the solvent on the **(a)** δ-Cu_2S and **(b)** β-Cu_2S, and the potential (i.e. limiting potential during the CO_2RR) of **(c)** −0.50 V (*vs* reversible hydrogen electrode (RHE)) on the δ-Cu_2S and **(d)** −0.39 V *vs*. RHE on β-Cu_2S. The model consists of a 3 × 3 × 1 supercell of δ-Cu_2S with 50 H_2O molecules, and β-Cu_2S with 28 H_2O molecules.